

## SUPPLEMENTARY INFORMATION

# Point Defects Modelling Explains Multiple Sulfur Species in Sulfur-doped $\text{Na}_4(\text{Al}_3\text{Si}_3\text{O}_{12})\text{Cl}$ Sodalite

Adrien Stoliaroff<sup>1</sup>, Romain Schira<sup>1</sup>, Féodor Blumentritt<sup>1</sup>, Emmanuel Fritsch<sup>1</sup>, Stéphane Jobic<sup>\*1</sup>,  
Camille Latouche<sup>\*1</sup>

<sup>1</sup>Université de Nantes, CNRS, Institut des Matériaux Jean Rouxel, IMN, F-44000 Nantes, France

[camille.latouche@cnrs-imn.fr](mailto:camille.latouche@cnrs-imn.fr)

[stephane.jobic@cnrs-imn.fr](mailto:stephane.jobic@cnrs-imn.fr)

## Computational details

### *Chemical potentials*

We propose herein a general algorithm to do it irrespectively from the number of chemical species composing the host compound.

As formalized in <sup>1</sup>, the stability domain is defined in terms of chemical potentials by:

$$(\mathcal{D}) \left\{ \begin{array}{l} \sum_{i=1}^N n_i^{\text{target}} \Delta \mu_i = \Delta H_f(\text{target}) \\ \forall i \in [1;N], \Delta \mu_i \leq 0 \\ \sum_{i=1}^N n_i^{\text{undesired}} \Delta \mu_i \leq \Delta H_f(\text{undesired}) \end{array} \right.$$

Where N is the total number of chemical species involved in the problem (host species + extrinsic defects). For instance in the case of sodalite,  $N = 5(\text{Al}, \text{Si}, \text{Na}, \text{O}, \text{Cl}) + 1 (\text{S}) = 6$  (extrinsic). The stability domain is a polyhedron in the chemical potential space of dimension N considered. Each of its summit is defined by the competition of the host and N-1 (here 5) competing compounds.

The algorithm to compute the summits is described in the following diagram. Before starting the post-process, the formation enthalpy of several competing compounds is computed *ab initio*. All the combinations of 5 compounds among the pool of 18 are tested following the steps described hereafter. A combination of 5 compounds is selected, in

competition with the host. It defines a matrix equation, which may possess a solution, *i.e.* a set of chemical potential values. To check whether this set of values lies in the stability domain of the host or not, it is tested against the system of inequations defined previously.

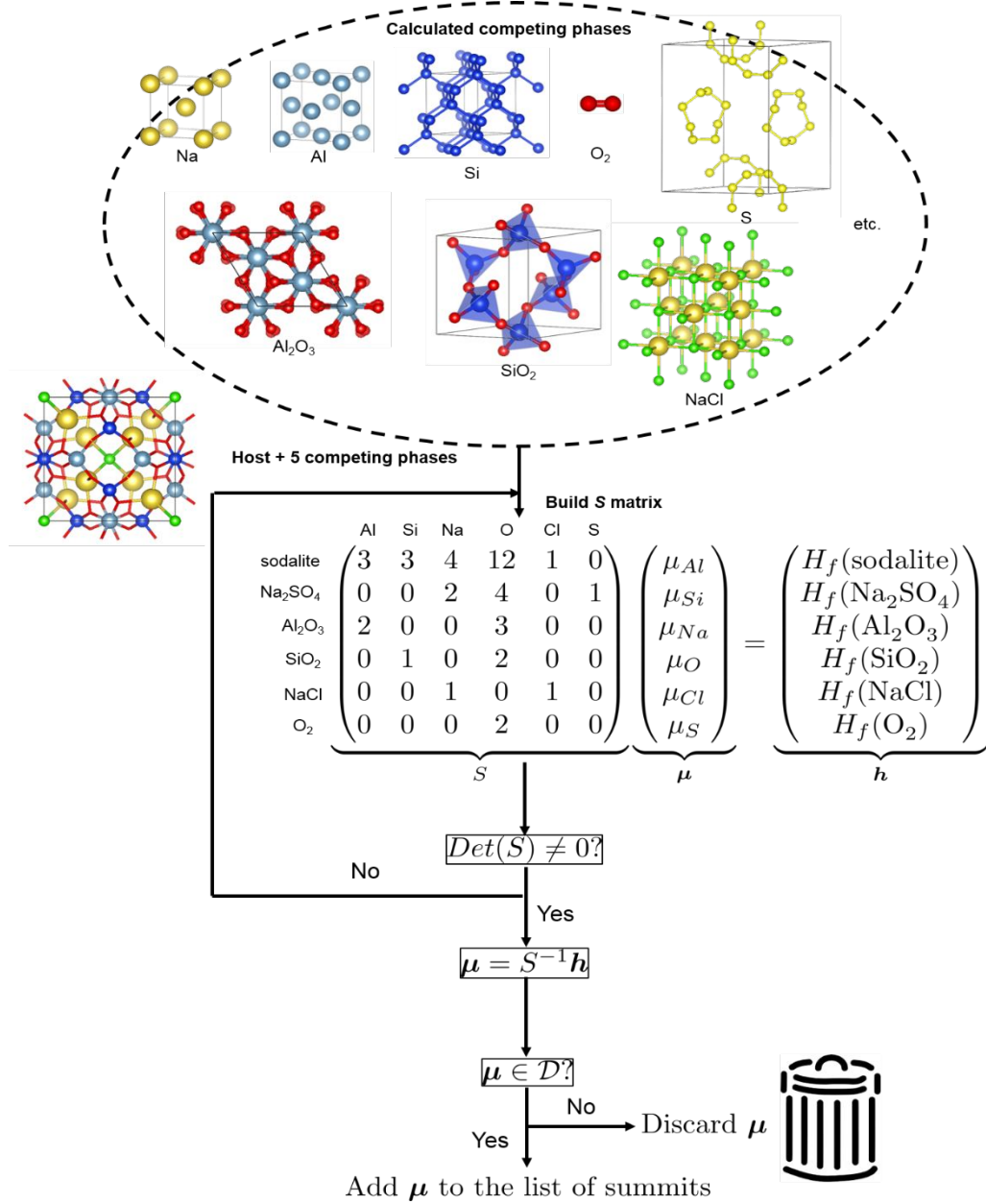


Figure S 1. Processus for the determination of the chemical potentials.

### Fermi level, effective masses and concentrations

The defect concentration  $n_{D,q}(E_F)$  of a defect D in charge state q can be approximated using Boltzmann distribution depending on the position of the Fermi level ( $E_F$ ) during synthesis, as expressed in:

$$n_{D,q}(E_F) \approx N \cdot \exp\left(\frac{-\Delta H_{\text{form}}^{D,q}(E_F)}{k_B T}\right)$$

where  $k_B$  is the Boltzmann constant,  $N$  is the number of sites available to the defect and  $T$  is the temperature of the synthesis. The entropic contribution to the Gibbs' free energy is considered negligible with respect to the enthalpy terms. The compound's charge is globally neutral, which sets the value of the Fermi energy so that the charges of the carriers (holes and electrons) and the defects compensate each other. Numerically, this is expressed as the following equation, the resolution of which leads to the determination of the Fermi level:

$$-n_e(E_F) + n_h(E_F) + \sum_D q_D \cdot n_{D,q_D}(E_F) = 0$$

Here,  $n_e(E_F)$  and  $n_h(E_F)$  are the concentrations of free electrons and holes, respectively, for a Fermi energy at a given temperature. They are given by the following equations:

$$n_e(E_F) = \int_{E_C}^{+\infty} g_e(\mu) \cdot f_{FD}(\mu - E_F) \cdot d\mu$$

and

$$n_h(E_F) = \int_{-\infty}^{E_V} g_h(\mu) \cdot (1 - f_{FD}(\mu - E_F)) \cdot d\mu$$

where  $f_{FD}(\mu - E_F)$  is the Fermi-Dirac function:

$$f_{FD}(\mu - E_F) = \frac{1}{1 + \exp\left(\frac{\mu - E_F}{k_B T}\right)}$$

and  $g_e(\mu)$  and  $g_h(\mu)$  are the density of states of respectively electrons and holes in 3D:

$$g_{e,h}(\mu) = \frac{1}{4\pi^2} \left( \frac{2m_{e,h}^*}{\hbar^2} \right)^{3/2} \sqrt{\mu}$$

*Table S 1. Number of  $N_D^{\text{sites}}$  with respect to the investigated defect.*

<b>Defects</b>	<b><math>N_D^{\text{sites}}</math></b>
V <sub>O</sub>	24
V <sub>Na</sub>	4
V <sub>Cl</sub>	2
S <sub>Cl</sub>	2
S <sub>2Cl</sub>	2
S <sub>3Cl</sub>	2
Al <sub>Si</sub>	6
Si <sub>Al</sub>	6

Table S 2. Experimental and computed structure parameters ( $\text{\AA}$ ). Relative deviation to experiment is given between brackets.

	Exp.	PBE	HSE06
$a = b = c$	8.870	8.930 (0.7%)	8.857 (-0.1%)
V ( $\text{\AA}^3$ )	698	712 (2%)	695 (-0.4%)
Na-Cl	2.730	2.736 (0.2%)	2.721 (-0.3%)
Al-O	1.728	1.761 (1.9%)	1.745 (1.0%)
Si-O	1.628	1.641 (0.8%)	1.624 (-0.2%)
Na-O	2.351	2.337 (-0.6%)	2.323 (-1.2%)

As one can see, the simulated cell parameters in PBE and in HSE06 are in very good agreement with respect to experiment. The fact that HSE06 is a more refined functional than PBE is respected. PBE slightly overestimates the cell's volume (2%) but the agreement remains correct with experimental data. Concerning the reported bond lengths in Table 1, one may assess that the simulations are well reproducing the experimental data obtained *via* X-ray diffraction..

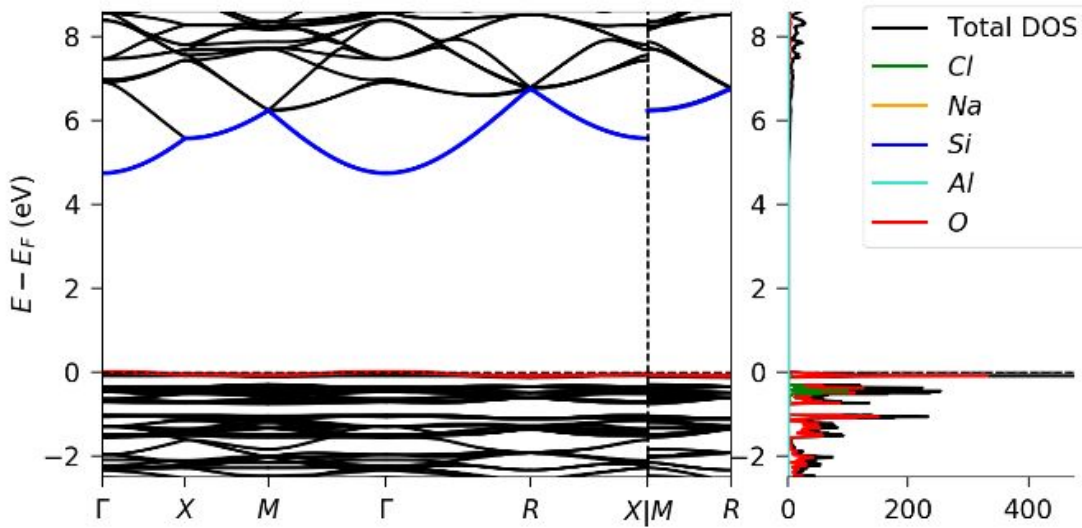


Figure S 2. Electronic band diagram and Density Of States (DOS) of sodalite computed with the PBE electronic density functional. The bandgap is direct in  $\Gamma$  (4.75 eV).

Table S 3. Computed Charge Transition Levels.

Defect	$\mu_{E_F}(\text{eV})$
$V_{Na}$	1.64
$Al_{Si}$	1.84
$SO_{4Cl}$	1.94
$V_O$	2.31
$S_{Cl}$	3.41
$S_{2Cl}$	4.61
$S_{3Cl}$	4.31
$V_{Cl}$	5.11
$Si_{Al}$	6.23

**References:**

- (1) Stoliaroff, A.; Jobic, S.; Latouche, C. PyDEF 2.0: An Easy to Use Post-Treatment Software for Publishable Charts Featuring a Graphical User Interface. *J. Comput. Chem.* **2018**, 39 (26), 2251–2261. <https://doi.org/10.1002/jcc.25543>.